Contents lists available at ScienceDirect

Transplant Immunology

A lectin affinity plasmapheresis device removes extracellular vesicles and microRNAs from renal perfusates following controlled oxygenated rewarming of discarded donor kidneys

Rosalia de Necochea Campion [*], Miguel Pesqueira, Paul Vallejos, Cameron McCullough, Alessio Bloesch, Steven P. LaRosa

Aethlon Medical Inc., 11555 Sorrento Valley Rd., San Diego, CA, United States of America

A B S T R A C T

Kidney transplantation is considered the benchmark treatment for end-stage kidney disease patients, yet the scarcity of suitable kidneys poses a significant hindrance for patients and healthcare providers. One approach is to extend the criteria for the use of kidneys from deceased brain death and deceased circulatory death donors. Use of these organs, especially from these extended criteria donors, is associated with ischemia reperfusion injury and resultant delayed graft function as well as increased rates of allograft rejection. To lessen these complications as well as increase the time of organ viability assessment, machine perfusion has been evaluated on recovered kidneys. In this study we examined the immunogenic molecular content of perfusates from discarded organs that had undergone Controlled Oxygenated Rewarming (COR). Perfusates were analyzed for extracellular vesicles (EVs), DNA (Deoxyribonucleic acid), and microRNAs. These perfusates were then pumped over a plasma separator containing a lectin affinity resin. Following treatment, a significant diminution in extracellular vesicles, dsDNA (double-stranded DNA) associated with EVs, and microRNAs (miRNA) were observed. Specifically, in three out of the four renal perfusates analyzed there was significant removal of small EVs (<200 nm) and vesicles loaded with dsDNA ($p < 0.05$). Notably, depletion of larger EVs (100-500 nm) was found to be significant in all treated perfusates ($p < 0.01$). NanoString analysis of miRNA found 5 species potentially involved in renal dysfunction (hsa-let 7a-5p, hsa-miR-148b-3p, hsa-miR-148a-3p, hsa-miR-29b-3pb and hsa-miR-99a5p) to be significantly depleted in treated renal perfusates ($p \leq 0.05$). These results support a future study incorporating this treatment method into a dynamic machine perfusion circuit to explore if reduction of these mediators is associated with improved function of retrieved kidneys.

1. Introduction

Renal transplantation has emerged as the gold standard treatment for end-stage kidney disease, offering a remarkable improvement in both the quality of life and life expectancy of patients [1]. However, there remains a significant shortage of available donor kidneys as well as a discard rate of approximately 25 % for those organs that are donated [2]. An unavoidable consequence of kidney donation from deceased donors is Ischemia Reperfusion Injury (IRI) as a result of renal artery clamping and cold ischemia associated with traditional static cold storage (SCS). Reperfusion injury leads to delayed graft function (DGF), defined as the need for dialysis in the first 7 days post-transplant, in approximately 30 % of renal transplant recipients with rates as high as 55 % seen with donors after circulatory death [3,4]. Delayed Graft Function is associated with poor future organ dysfunction as well as allograft rejection [4].

An advance in the field has been the use of ex vivo machine perfusion of recovered kidneys in the place of traditional static cold storage.

Hypothermic Machine Perfusion (HMP) is associated with lower rates of DGF compared with standard cold storage (SCS) in the setting of renal transplantation [5]. Consideration has now been given as to whether Controlled Oxygenated Rewarming (COR) with a period of end-normothermic machine perfusion (NMP) may have advantages over HMP. One potential advantage of gradual rewarming would be less mitochondrial damage and resultant ischemia reperfusion injury [6]. A second potential benefit of this approach is to provide additional time to assess organs and determine viability rather than discard for excessive cold ischemia time [7].

Early studies with Controlled Oxygenated Rewarming with a period of normothermic machine perfusion by Minor and colleagues have been performed demonstrating its' feasibility [8,9]. A definitive trial with the Minor protocol has not been published to date. The largest clinical trial done to date incorporating a period of normothermic machine perfusion did not demonstrate a benefit compared to static cold storage on DGF rates of recovered kidneys [10]. A few observations that have been made during NMP may explain this lack of benefit. First, release of extracellular vesicles, which have been implicated in ischemia reperfusion injury [11] have been noted to be released during normothermic renal perfusion [12]. Second, inflammatory cytokine release has been noted during NMP [13]. Finally, endothelial damage and the development of microthrombi have been noted during NMP as well [14]. All these findings suggest that the addition of a device that removes inflammatory mediators to a COR circuit might be a valuable adjunct to this treatment of retrieved kidneys.

The Aethlon Hemopurifier is one such device that could serve to remove extracellular vesicles and microRNAs released during the course of COR with NMP. The Hemopurifier (HP) is a combination therapeutic device with a hollow fiber 0.2 µm filter, and an affinity resin produced with a lectin derived from the *Galanthus nivalis* plant (the common snowdrop). The Hemopurifier was designed as an extracorporeal device to be used in blood purification. It combines plasma separation, size exclusion and affinity binding of structures containing mannose [15]. Extracellular vesicles have previously been noted to bind the *Galanthus nivalis agglutinin* lectin in the affinity resin of the Hemopurifier [16]. The Hemopurifier has previously been demonstrated to remove extracellular vesicles from cancer patients when spiked into a buffer solution in vitro [17] and from a patient with severe COVID-19 infection in vivo [15]. Exosomal miRNAs associated with coagulopathy and acute lung injury were also removed during treatment. In this described proof of concept experiment we examined the ability of the Hemopurifier to remove EVs and microRNAs from perfusate samples collected upon completion of Controlled Oxygenated Rewarming of discarded donor kidneys.

1.1. Objective

Measure the ability of the Hemopurifier to remove donor EVs, DNA, and microRNAs in renal perfusates from kidneys perfused with a controlled oxygenated rewarming (COR) protocol.

2. Materials and methods

2.1. Ethics statement

Four human kidneys from the United Network for Organ Sharing (UNOS) program, deemed unsuitable for transplantation, were included in this study. Kidneys discarded for transplantation were offered to 34 Lives by non-profit Organ Procurement Organizations (OPOs). Consent to use these donor kidneys for research was acquired by the OPOs in adherence to standards outlined in the Uniform Anatomical Gift Act of the United States.

2.2. Controlled Oxygenated Rewarming (COR) with End Normothermic Machine Perfusion (NMP)

Discarded kidneys, which had been previously placed on preservation protocols (hypothermic machine perfusion preservation or static cold storage preservation) were perfused with a controlled oxygenated rewarming (COR) protocol designed at 34 Lives (West Lafayette, IN) from an adaptation of the Minor protocol [8]. A mixture of a 750 mL of Steen™ solution (XVIVO Perfusion, Gothenburg, Sweden) and 750 mL of Ringer's Lactate solution was used as the perfusate, after adding 10 mL of 8.4 % Sodium Bicarbonate, 7 mL of 10 % Calcium Gluconate, 1 g of ampicillin, and 500 mg of ceftriaxone. The initial 5 °C temperature was gradually increased to 10 °C, 17 °C, 30 °C, and 35 °C at timepoint intervals of 30, 60, 75, and 90 min. The perfusion flow rate was adjusted to achieve incremental targeted arterial pressure from 30 to 75 mmHg in the final state period at 35 °C. An oxygenator was set to maintain a partial pressure of oxygen above 500 mmHg ensuring adequate oxygen supply to the organ during the final perfusion stage at 35 °C. Total near normothermic perfusion time was 2 h. Subsequentially, the cumulative renal perfusate solution was collected, frozen, and shipped to Aethlon Medical where they were stored at −80 °C until thawed for further analysis.

2.3. Hemopurifier GNA Lectin-Affinity Treatment of Renal Perfusates

A 250 mL volume of COR treated renal perfusate was circulated through the HP cartridge circuit at 200 mL/min using a Spectrum Kr21 peristaltic pump system for a total of 24 volume passes (Fig. 1). Each HP cartridge contained 40 g of *Galanthus nivalis* agglutinin (GNA) affinity resin (Aethlon Lot No. RD070523). As shown in Fig. 1, during HP treatment the kidney perfusate passes through the packed column of GNA affinity resin promoting molecular interactions between the donor renal perfusate and the resin.

2.4. EV quantification

Concentration of EV and dsDNA-associated EV nanoparticles was determined through the use of high sensitivity nanoparticle NanoFCM Flow Analyzer U30 (NanoFCM, Nottingham, UK). Co-staining was performed by first mixing samples directly with 2 µM MemGlow 640 nm (MemGlow™ 640: Fluorogenic Membrane Probe, Cytoskeleton) at a 1:1 ratio for quantification of EV particles. 2 µL of MemGlow stained sample was diluted into 98 µL of reverse osmosis (RO) purified water (Sartorius) and stained with SYTOX Green Ready Flow Reagent (Invitrogen), a membrane impermeable nucleic acid dye. The nucleic dye itself was diluted 10-fold, used to stain at a ratio of 1:1 with the diluted MemGlow stained sample and incubated at room temperature for 15 min prior to single event counting analysis on the NanoFCM instrument.

2.5. RNA isolation

Total RNA was isolated from both pre- and post-HP circulated kidney perfusates. The RNA isolation kit used was the Plasma/Serum RNA purification Mini Kit (Norgen Biotek Corp, Thorold, Canada) according to the manufacturer's protocol. In brief, 200 µL of kidney perfusate were thoroughly mixed with the lysis buffer and three spike-in exogenous miRNAs were added (ath-miR159a, cel-miR-248, osa-miR414) at a 1.6 pM concentration before processing on the spin column. Purified RNA was eluted with 20 µL of elution buffer and quantified using the Nanodrop One Spectrophotometer (ThermoFisher Scientific).

2.6. NanoString nCounter miRNA assay

A 10 µL aliquot of purified RNA (~25 ng/µL) from each sample was provided to the NanoString Services Laboratory at Canopy Biosciences (Canopy Biosciences, Hayward, CA). The samples were prepared for
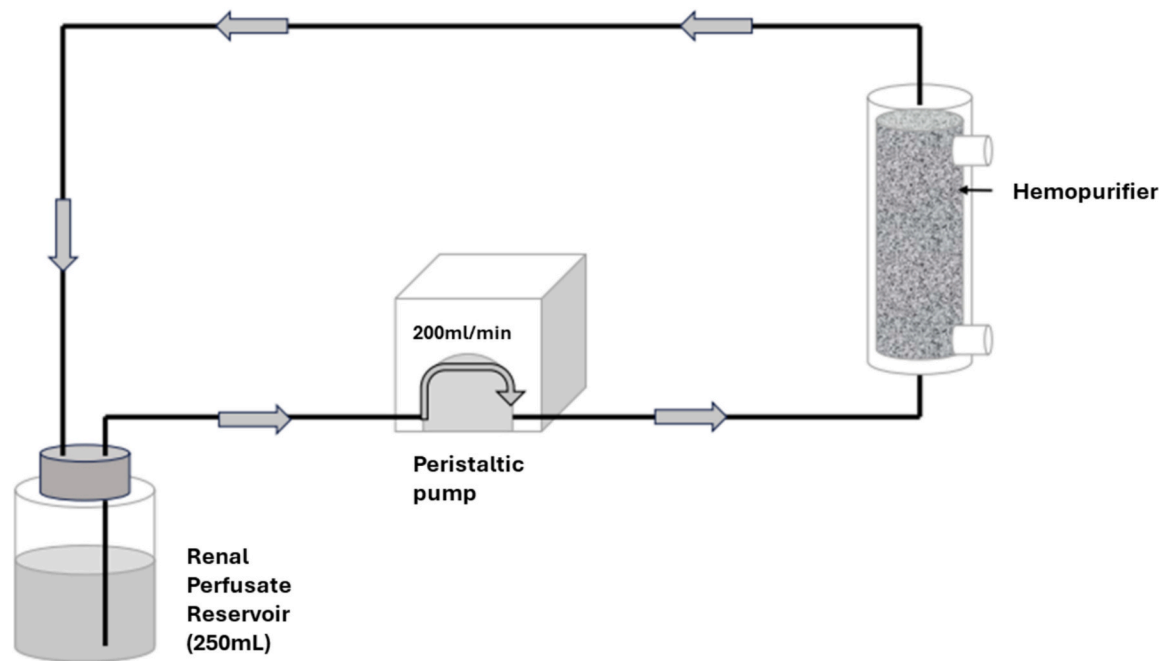
Fig. 1. Renal Perfusate Hemopurifier Treatment Circuit. This figure depicts the benchtop configuration of the circuit used to treat the kidney perfusates with the Hemopurifier cartridge. Kidney perfusates were circulated through the Hemopurifier where they passed through a packed column of GNA affinity resin for a total of 24 cycles (30 min). Perfusate samples were collected after treatment and compared to pre-treatment samples to identify differences in EV and miRNA contents.

NanoString nCounter miRNA expression profiling according to the manufacturer's protocol. Analysis of miRNA raw data (RCC data files) was performed using the NanoString nSolver analysis software (version 4.0). This R-based software package is the only tool that allows for data normalization using the NanoString ligation controls, in addition to its other important analytical elements including signal density quality controls, background correction, and differential expression analysis [18]. Before data normalization, background thresholding was performed, setting the threshold count value to 25 reads based on the mean count of the negative controls plus two standard deviations. Data normalization was performed using the geometric mean of the exogenous spike-in miRNA values (ath-miR159a, cel-miR-248, osa-miR414) in addition to the nCounter positive ligation controls. Differential analysis was then performed to assess miRNA targets significantly altered by Hemopurifier treatment.

2.7. Statistical analysis

Statistical analyses on extracellular vesicle data sets was performed using GraphPad Prism 8 software. A one-tailed paired t-test was used to assess significant changes in the EV measurements between treatment groups. The accepted level of significance was $P \leq 0.05$ indicated by one asterisk (see figure legends). Statistical analysis of the miRNA datasets was performed using the NanoString nSolver analysis software (version 4.0) to identify significant changes in treated perfusate samples. The nSolver False Discovery Rate (FDR) filter was applied to control for error in multiple hypothesis p-values testing and identify only those changes that were truly significant in this treatment model. Significance was defined as $p \leq 0.05$.

3. Results

3.1. Donor characteristics

HP treated perfusates were obtained from four different deceased renal donors (2 DCD and 2 DBD) with a median Kidney Donor Patient Index (KDPI) of 75.5 %, ranging from moderate to high risk of graft

rejection/function [19]. Median Cold ischemia time was 28 h and 12 min and other health and demographic data contributing to the calculated KDPI values is shown in Table 1.

3.2. Extracellular vesicles and a DNA-associated subpopulation of these nanoparticles are depleted by Hemopurifier treatment
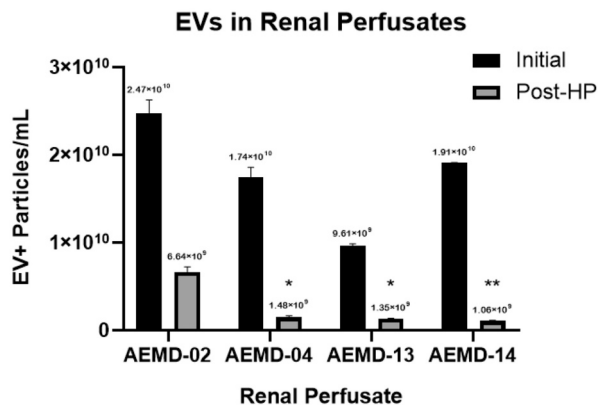
Nanoparticle flow cytometry analysis of renal perfusates was performed to quantify the concentrations of small EVs, 40–200 nm size range, and larger EVs in the 100–500 nm range pre- and post- HP treatment. Although small EVs and larger EVs inherently have some size overlap, it is important to distinguish between these subpopulations because they are known to have different cellular biogenesis origins and distinct cargo with different implications in renal transplant outcomes [20,21].

As shown in Fig. 2a, there is a statistically significant reduction of

Table 1
Renal donor characteristics and demographics.

| Perfusate	(AEMD-02)	(AEMD-04)	(AEMD-13)	(AEMD-14)
Age (y)	69	64	26	58
Gender	M	M	M	F
Ethnicity	White	Black or African American	Black or African American	White
Cause of death	Hemorrhagic Stroke	Ischemic Stroke	Anoxic brain injury	Anoxic brain injury
DCD/DBD	DCD	DBD	DBD	DCD
KDPI	97 %	96 %	24 %	55 %
Cold Ischemic time (HH:mm)	21:14	25:27	30:57	58:24
History of Hypertension	Yes	Yes	No	No
BMI (Kg/m^2)	32.38	22.96	27.42	26.50
Initial organ weight (g)	630	229	276	516
s/p CPR	No	No	Yes	Yes

A.

B.
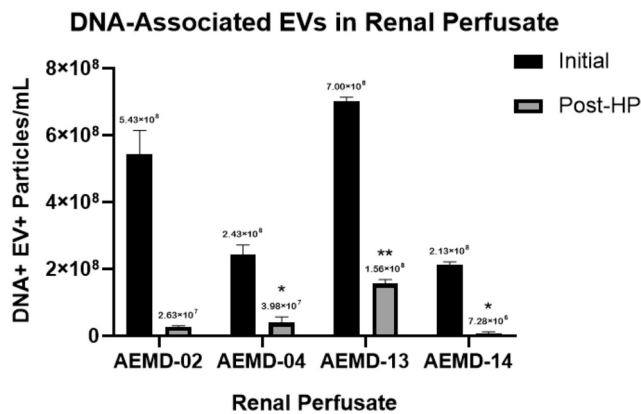
Fig. 2. Renal perfusates contain small extracellular vesicles that are removed by Hemopurifier treatment. (A) NanoFCM nanoparticle flow cytometry analysis demonstrates that the Hemopurifier removes the majority of small EV particles (40-200 nm nanovesicles) and (B) of dsDNA loaded EV particles in treated renal perfusates. The data shown represents the mean and standard error of 2 technical replicates measured from each perfusate sample. (* $p \leq 0.05$; **$p \leq 0.01$).

small EV particles in 3 out of 4 of the HP treated renal perfusates. For example, AEMD-04 had a measured average initial concentration of 1.74E+10 EV particles/mL and a post-HP treatment concentration of 1.48E+9 EV particles/mL, signifying over a 10-fold significant reduction. In contrast, although EV reduction was nearly 4-fold in AEMD-02 treated perfusates, this difference did not quite reach statistical significance ($p = 0.052$). Comparison of pre- and post-HP small EV particles/mL (40–200 nm size) from AEMD-02, AEMD-04, AEMD-13, and AEMD-14 perfusates demonstrate a 73.1 %, 91.5 %, 86.0 %, and 94.5 % vesicle depletion, respectively. Further, particle co-localization quantification analysis for EVs in tandem with dsDNA showed a significant reduction, of similar extent to the EV depletion, of this DNA-associated EV subpopulation across the four renal perfusate samples, as shown in Fig. 2b. The small DNA-associated EV particle concentrations of AEMD-02. AEMD-04, AEMD-13, and AEMD-14 perfusates were depleted by 95.2 %, 84.9 %, 77.7 %, and 96.4 %, respectively. These reductions were all found to be statistically significant (Fig. 2b), except for AEMD-02 where the difference did not quite reach statistical significance ($p = 0.058$).

To gain further insight into the HP's ability to remove EVs from renal perfusates, we adjusted our nanoparticle flow cytometry parameters for the detection of larger EVs ranging from 100 to 500 nm in diameter size. Although the quantity of EVs in the 100–500 nm size range in the renal perfusates samples is less abundant than those in the 40–200 nm range,

there is also statistically significant reduction of these larger EVs by the HP treatment. As shown in Fig. 3a, these larger EV populations were all significantly reduced by 94.6 %, 98.9 %, 71.0 %, and 99.4 % in the AEMD-02, AEMD-04, AEMD-13, and AEMD-14 perfusate samples, respectively. Moreover, the subpopulation of DNA-associated larger EVs was also significantly reduced, as shown in Fig. 3b, with an average depletion of 98.2 %, 100 %, 89.7 %, and 100 % for each of the four renal perfusate samples, respectively.

3.3. Perfusate miRNAs are depleted by hemopurifier treatment

Pre- and post-HP treated RNA was submitted for miRNA analysis. Out of the potential 798 miRNAs present on the NanoString Human miRNA Panel, 341 miRNAs were detected in the perfusate with content levels that could be measured above the background threshold. Of those 341 detectable miRNAs, 235 were depleted by HP treatment (data not shown). Initially, 22 of these miRNAs were found to be significantly
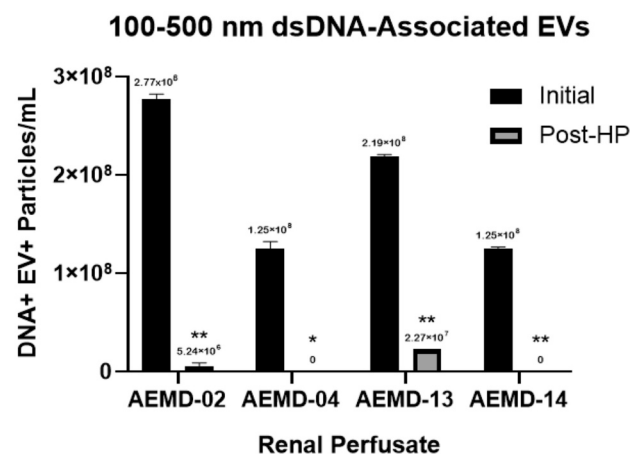
A.
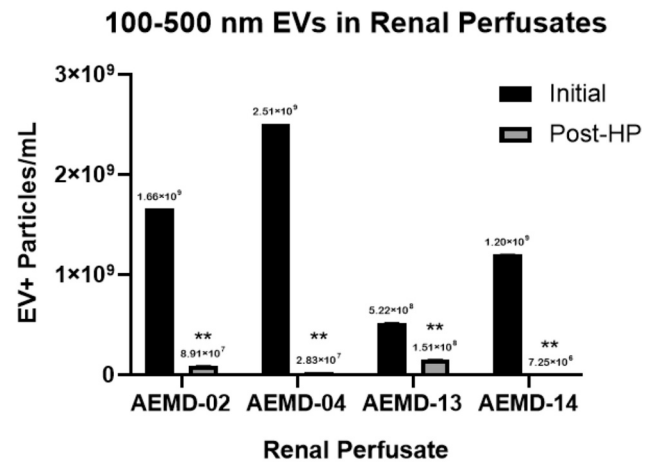
B.

Fig. 3. Larger extracellular vesicles within the fiber pore-size filtration capacity of the Hemopurifier are removed from treated renal perfusates. (A) Differences in 100–500 nm EV counts from the four treated renal perfusates. (B) pre- and post-HP concentrations of DNA-associated large EV particles. Measurements for AEMD-04 and AEMD-14 post-HP DNA-associated EV particles were below the instrument's limit of detection which was 5.22E+6 and 5.58E+6/mL, respectively. Data shown represent the mean and standard error of 2 technical replicates measured from each perfusate sample. (* p ≤ 0.05; ** p ≤ 0.01).

depleted ($p < 0.05$) by treatment (Supplemental Table 1). However, when a false discovery rate filter was applied to the data to control for the type I error in our multiple testing model, we found that only 5 of these miRNA were identified as significantly reduced by HP treatment (Table 2). The average reduction in this group was 67.8 % with species such as hsa-let-7a-5p and hsa-miR-29b-3p demonstrating the highest levels of 86.5 % and 77.7 % depletion, respectively.

4. Discussion

This study has provided significant insights into the release of extracellular vesicles and microRNAs during Controlled Oxygenated Rewarming with end near- Normothermic Machine Perfusion (NMP). Importantly, we observed large quantities of extracellular vesicles, EVs with DNA cargo, and microRNAs released during the procedure. Furthermore, the Aethlon Hemopurifier® removed these potential donor organ transplant mediators from the end perfusate. This data raises the hypothesis that incorporation of the device into the COR treatment of a recovered kidney might improve viability of extended criteria kidneys and important outcomes following kidney transplantation.

Extracellular vesicles or EVs are heterogenous lipid bilayer membrane nanoparticles (20–10,000 nm in diameter) released by all cell types that participate in cell-to-cell communication [22]. Within the EVs are cargo including nucleic acids, proteins, cytokines and non-coding microRNAs involved in regulation of transcription. Extracellular vesicles released as a consequence of hypoxia have been implicated in ischemia reperfusion injury as well as Delayed Graft Function [11]. Donor derived EVs have also been implicated in the development of allograft rejection [23]. Woud et al. is but one group that demonstrated an increase in EV number during the course of normothermic machine perfusion in extended criteria donor discarded kidneys [12]. Rutman et al. examined hypothermic kidney perfusate EVs and found that they were < 500 nm in diameter and that they contained donor HLA markers [24]. We were able to demonstrate a 73 % to 94 % reduction in total EV concentration when renal perfusates were run over the Aethlon Hemopurifier. Furthermore, we were able to demonstrate removal of EVs up to 500 nm in size (Supplemental Fig. 1). This larger size range is known to include donor microvesicles and apoptotic bodies with distinct molecular cargo which can contribute to graft dysfunction [21].

The nanoparticle flow cytometry analysis results also demonstrate the Aethlon Hemopurifier's ability to remove dsDNA-associated EVs from renal perfusates. The small EVs (40–200 nm in diameter) most likely contain dsDNA molecules associated to their surface due to the membrane-impermeable nature of the Sytox green nucleic acid dye co-localized with the phospholipid bilayer stain. Although the mechanism through which this occurs is not well understood, this phenomenon has been observed in other small EV populations and might be worth exploring further [25]. More importantly though, DNA from EVs can induce the recruitment of immune cells in various conditions by incrementing the expression of type I interferons and cytokines through the activation of the DNA damage receptor cyclic GMP-AMP synthase (cGAS)-stimulator of interferon genes (STING) pathway [25,26]. Therefore, the elimination of dsDNA-associated EVs in renal perfusates by HP treatment suggests another therapeutic mechanism to reduce inflammation and immune response after transplantation.

One specific cargo component of extracellular vesicles that has garnered attention in renal perfusates is microRNAs. Gremmels et al. specifically examined renal donor preservation fluid and found 10 kidney perfusate extracellular vesicle (KP-EV) miRNAs that differentiated delayed graft function from immediate graft function [27]. In the study by Rutman he found increased levels of miRNA 218-5p that was associated with delayed graft function as a result of an increased TH17 /T regulatory cell ratio [24]. In separate studies, Li and Ding have identified exosomal miRNAs associated with renal ischemia/reperfusion injury that could be blocked by antagonist treatment [28,29]. This data in total raises the possibility that EV miRNAs could be targets for removal during machine perfusion of recovered kidneys.

Our study examined the largest number of microRNAs in perfusates to date following normothermic machine perfusion of discarded kidneys. After controlling for false discovery, we observed a significant reduction in five microRNAs after the perfusates were passed over the Hemopurifier. The Aethlon Hemopurifier® treatment led to the significant depletion of hsa-let-7a-5p, hsa-miR-148b-3p, hsa-miR-148a-3p, hsa-miR-29b-3pb and hsa-miR-99a5p. These data appear to suggest that the mechanism of miRNA removal is affinity based and that miRNA species with significant depletion may be packaged in EVs with specific mannose-rich glycosylation patterns. Let-7a-5p has been found to be a regulator promoting renal dysfunction. Upregulation has been noted in Multiple Myeloma patients [30]. Inhibition of the let-7a/TGFCR1 signaling has ameliorated diabetic nephropathy while let-7a upregulation has been demonstrated to enhance hyperinflammation by increasing cell proliferation and NFkappa-b activation in SLE cell models [31,32]. In prior studies miR-148b-3p has been associated with IgA nephropathy [33]. Upregulation of this microRNA has been seen in localized irradiation injury in a mouse model and following LPS injection in a pig model [34,35]. The microRNA 148a-3p has been associated with renal fibrosis in a unilateral ureteral ligation model [36]. Additionally, miR-148a-3p has been shown to promote polarization to an inflammatory M1 phenotype in macrophages as well as be involved in pro-inflammatory cytokine release [37,38]. The miR-29b-3p has been noted to be upregulated in renal chronic allograft patients but its role may be protective and not injurious [39]. Finally, miR-99a-5p has been associated with urinary EVs in renal ANCA-associated vasculitis but has an unclear role in renal diseases [40].

Despite the promising findings of this study there are limitations to consider. The study was done with spent renal perfusates following the completion of the COR treatment. As such we did not examine the kinetics of production or removal of these EVs and microRNAs over the course of the Hemopurifier treatment. Additionally, we do not know the effects on the histopathology of the recovered organ or the effects of removal of these mediators on renal function. We also only studied effects on perfusates following a COR protocol while Hypothermic Machine Perfusion is the current standard of care for ex vivo treatment of recovered kidneys. The next step would be to compare mediator removal, renal function and histopathology in a COR circuit performed with or without incorporation of the Hemopurifier on discarded kidneys. Ultimately, we would need a clinical trial demonstrating that incorporation of the Hemopurifier into renal perfusion improves important clinical endpoints in transplant recipients such as DGF, graft survival or rejection rates to justify its use.

Disclosure statement

All authors of this manuscript were employed by Aethlon Medical, the manufacturer of the Hemopurifier during the preparation of this manuscript.

The findings reported in this manuscript were initially disclosed on

Table 2
Significantly depleted miRNA in Hemopurifier treated perfusates.

Probe Name	Accession #	24P vs. ctrl	FDR (p-value)	Percent Reduction
hsa-let-7a-5p	MIMAT0000062	−7.4	0.00	−86.5
hsa-miR-148b-3p	MIMAT0000759	−1.78	0.04	−43.7
hsa-miR-148a-3p	MIMAT0000243	−2.36	0.04	−57.7
hsa-miR-29b-3p	MIMAT0000100	−4.48	0.05	−77.7
hsa-miR-99a-5p	MIMAT0000097	−3.75	0.05	−73.3

August 24, 2024 on the preprint server BioRxiv [41]. (https://doi.org/10.1101/2024.08.23.609252).

CRediT authorship contribution statement

Rosalia de Necochea Campion: Writing – review & editing, Writing – original draft, Supervision, Methodology, Investigation, Formal analysis. **Miguel Pesqueira:** Writing – review & editing, Writing – original draft, Resources, Methodology, Formal analysis, Data curation. **Paul Vallejos:** Writing – original draft, Supervision, Investigation, Formal analysis. **Cameron McCullough:** Writing – original draft, Resources, Investigation. **Alessio Bloesch:** Writing – original draft, Investigation. **Steven P. LaRosa:** Writing – review & editing, Writing – original draft, Supervision, Resources, Conceptualization.

Acknowledgments

Appendix A. Supplementary data

Supplementary data to this article can be found online at https://doi.org/10.1016/j.trim.2025.102215.

Data availability

The raw data supporting the conclusions of this article will be made available by the authors upon request.

References

[1] R. Zulpaite, et al., Ex-vivo kidney machine perfusion: therapeutic potential, Front Med (Lausanne) 8 (2021) 808719.
[2] S. Mohan, et al., Increasing discards as an unintended consequence of recent changes in United States kidney allocation policy, Kidney Int. Rep. 8 (5) (2023) 1109–1111.
[3] C.J. Wang, J.B. Wetmore, A.K. Israni, Old versus new: Progress in reaching the goals of the new kidney allocation system, Hum. Immunol. 78 (1) (2017) 9–15.
[4] T.J. Zens, et al., The impact of kidney donor profile index on delayed graft function and transplant outcomes: a single-center analysis, Clin. Transpl. 32 (3) (2018) e13190.
[5] S.J. Tingle, et al., Machine perfusion preservation versus static cold storage for deceased donor kidney transplantation, Cochrane Database Syst. Rev. 3 (3) (2019) CD011671.
[6] H. Zlatev, C. von Horn, T. Minor, Preservation of mitochondrial coupling and renal function by controlled oxygenated rewarming of porcine kidney grafts, Biomolecules 11 (12) (2021).
[7] S.A. Hosgood, et al., Normothermic machine perfusion for the assessment and transplantation of declined human kidneys from donation after circulatory death donors, Br. J. Surg. 105 (4) (2018) 388–394.
[8] T. Minor, et al., First-in-man controlled rewarming and normothermic perfusion with cell-free solution of a kidney prior to transplantation, Am. J. Transplant. 20 (4) (2020) 1192–1195.
[9] H. Zlatev, et al., Clinical use of controlled oxygenated rewarming of kidney grafts prior to transplantation by ex vivo machine perfusion. A pilot study, Eur. J. Clin. Investig. 52 (2) (2022) e13691.
[10] S.A. Hosgood, et al., Normothermic machine perfusion versus static cold storage in donation after circulatory death kidney transplantation: a randomized controlled trial, Nat. Med. 29 (6) (2023) 1511–1519.
[11] X. Zhao, et al., Role of extracellular vesicles in pathogenesis and therapy of renal ischemia-reperfusion injury, Biomed. Pharmacother. 165 (2023) 115229.
[12] W.W. Woud, et al., Extracellular vesicles released during Normothermic machine perfusion are associated with human donor kidney characteristics, Transplantation 106 (12) (2022) 2360–2369.
[13] J.R. Ferdinand, et al., Cytokine absorption during human kidney perfusion reduces delayed graft function-associated inflammatory gene signature, Am. J. Transplant. 21 (6) (2021) 2188–2199.
[14] T.M. Huijink, et al., Loss of endothelial Glycocalyx during Normothermic machine perfusion of porcine kidneys irrespective of pressure and hematocrit, Transplant. Direct 9 (8) (2023) e1507.
[15] D.E. Amundson, et al., Removal of COVID-19 spike protein, whole virus, exosomes, and Exosomal MicroRNAs by the Hemopurifier(R) lectin-affinity cartridge in critically ill patients with COVID-19 infection, Front Med (Lausanne) 8 (2021) 744141.
[16] B.S. Batista, et al., Identification of a conserved glycan signature for microvesicles, J. Proteome Res. 10 (10) (2011) 4624–4633.
[17] A.M. Marleau, et al., Abstract 4509: targeting tumor-derived exosomes using a lectin affinity hemofiltration device, Cancer Res. 80 (16_Supplement) (2020) 4509.
[18] J. Chilimoniuk, et al., Challenges and opportunities in processing NanoString nCounter data, Comput. Struct. Biotechnol. J. 23 (2024) 1951–1958.
[19] Q. Bachmann, et al., The kidney donor profile index (KDPI) correlates with histopathologic findings in post-reperfusion baseline biopsies and predicts kidney transplant outcome, Front Med (Lausanne) 9 (2022) 875206.
[20] J. Ashcroft, et al., Extracellular vesicles in kidney transplantation: a state-of-the-art review, Kidney Int. 101 (3) (2022) 485–497.
[21] L. Ramalhete, et al., Exosomes and microvesicles in kidney transplantation: the long road from trash to gold, Pathology 56 (1) (2024) 1–10.
[22] W. Phillips, E. Willms, A.F. Hill, Understanding extracellular vesicle and nanoparticle heterogeneity: novel methods and considerations, Proteomics 21 (13–14) (2021) e2000118.
[23] W.W. Woud, et al., Direct detection of circulating donor-derived extracellular vesicles in kidney transplant recipients, Sci. Rep. 12 (1) (2022) 21973.
[24] A.K. Rutman, et al., Extracellular vesicles from kidney allografts express miR-218-5p and Alter Th17/Treg ratios, Front. Immunol. 13 (2022) 784374.
[25] E.Z. Malkin, S.V. Bratman, Bioactive DNA from extracellular vesicles and particles, Cell Death Dis. 11 (7) (2020) 584.
[26] Q. Chen, L. Sun, Z.J. Chen, Regulation and function of the cGAS-STING pathway of cytosolic DNA sensing, Nat. Immunol. 17 (10) (2016) 1142–1149.
[27] H. Gremmels, et al., The small RNA repertoire of small extracellular vesicles isolated from donor kidney preservation fluid provides a source for biomarker discovery for organ quality and Posttransplantation graft function, Transplant. Direct 5 (9) (2019) e484.
[28] C. Ding, et al., Exosomal MicroRNA-374b-5p from tubular epithelial cells promoted M1 macrophages activation and worsened renal ischemia/reperfusion injury, Front. Cell Dev. Biol. 8 (2020) 587693.
[29] Z.L. Li, et al., HIF-1alpha inducing exosomal microRNA-23a expression mediates the cross-talk between tubular epithelial cells and macrophages in tubulointerstitial inflammation, Kidney Int. 95 (2) (2019) 388–404.
[30] D. Ren, Y. Cai, G. Xu, Potential of microRNA expression profile in predicting renal impairment risk in multiple myeloma patients, Transl. Cancer Res. 9 (3) (2020) 1495–1505.
[31] P. Venugopal, et al., Differential expression of microRNAs let-7a, miR-125b, miR-100, and miR-21 and interaction with NF-kB pathway genes in periodontitis pathogenesis, J. Cell. Physiol. 233 (8) (2018) 5877–5884.
[32] N. Yan, et al., Naringenin ameliorated kidney injury through let-7a/TGFBR1 signaling in diabetic nephropathy, J. Diabetes Res. 2016 (2016) 8738760.
[33] S. Kumar, et al., miR-148b as a potential biomarker for IgA nephropathy, Kidney Dialysis 3 (1) (2023) 84–94.
[34] L. Ancel, et al., microRNA blood signature for localized radiation injury, Sci. Rep. 14 (1) (2024) 2681.
[35] J. Zhang, et al., Analysis of MicroRNA expression profiles in weaned pig skeletal muscle after lipopolysaccharide challenge, Int. J. Mol. Sci. 16 (9) (2015) 22438–22455.
[36] X. Li, et al., Screening and identification of key microRNAs and regulatory pathways associated with the renal fibrosis process, Mol. Omics 18 (6) (2022) 520–533.
[37] J. Amin Mohedin, et al., Resolvin D1 (Rvd1) attenuates in vitro LPS-stimulated inflammation through downregulation of miR-155, miR −146, miR −148 and Krupple like factor 5, Rep. Biochem. Mol. Biol. 12 (4) (2024) 566–574.
[38] F. Huang, et al., miR-148a-3p mediates notch signaling to promote the differentiation and M1 activation of macrophages, Front. Immunol. 8 (2017) 1327.
[39] Y.J. Chen, et al., Association between circulating MicroRNAs (miR-21-5p, miR-20a-5p, miR-29b-3p, miR-126-3p and miR-101-3p) and chronic allograft dysfunction in renal transplant recipients, Int. J. Mol. Sci. 23 (20) (2022).
[40] J. Frydlova, et al., Analysis of microRNAs in small urinary extracellular vesicles and their potential roles in pathogenesis of renal ANCA-associated Vasculitis, Int. J. Mol. Sci. 23 (8) (2022).
[41] R. de Necochea Campion, et al., The Hemopurifier removes extracellular vesicles and microRNAs from renal perfusates following controlled oxygenated rewarming of discarded donor kidneys, bioRxiv (2024), https://doi.org/10.1101/2024.08.23.609252, p. 2024.08.23.609252.